27th EPS Conference on Contr. Fusion and Plasma Phys. Budapest, 12-16 June 2000 ECA Vol. **24B** (2000) 324 -327

FULL SPECTRUM STABILITY ANALYSIS OF THE TOKAMAK EDGE REGION

P.B. Snyder, H.R. Wilson,[1] X.Q. Xu,[2] J.R. Ferron, L.L. Lao, M.S. Chu, E.J. Strait, and A.D. Turnbull

General Atomics, P.O. Box 85608, San Diego, California
[1]EURATOM/UKAEA Fusion, Culham Science Centre, Abingdon, United Kingdom.
[2]Lawrence Livermore National Laboratory, Livermore, California.

Tokamak performance is strongly tied to the stability and transport properties of the edge plasma. In many transport models, the height of the edge pressure "pedestal" essentially determines overall plasma confinement. Theoretical analysis of edge instabilities which may control the pedestal height and width is complex, in part because the sharp pressure gradients, and consequent large bootstrap currents, near the H–mode edge can destabilize kink, peeling, and ballooning modes over a wide range of toroidal mode numbers (n). Additional complications arise from separatrix geometries and non-ideal physics.

Ideal MHD stability studies of edge localized modes (ELMs) and experimentally observed ELM precursors suggest an important role for instabilities in the intermediate range of mode numbers ($3 \lesssim n \lesssim 30$). Continuing improvements in algorithms and computation speed have allowed low-n stability codes to treat a growing extent of the lower end of this range ($n \lesssim 10$) [1]. Higher values of n have traditionally been studied via ballooning theory. An important modification of classical ballooning theory has recently been developed, allowing proper treatment of the coupled system of edge ballooning and peeling modes [2,3]. This edge ballooning formalism has been studied in both shifted circle and shaped local equilibrium geometry [2,3,4], leading to the development of a model for the ELM cycle, and to insight about the role of second stability in the edge region.

Here we solve the edge ballooning/peeling equations in general, nonlocal tokamak geometry, using an enhanced version of the ELITE code. The nonlocal equilibrium allows proper treatment of both strongly edge-localized and more extended modes, for all plasma shapes. In conjunction with low-n MHD codes, this allows the study of the ideal MHD edge stability of real tokamak equilibria over essentially the full spectrum of toroidal modes. Important caveats are that ELITE keeps only the dominant [up to $O(n^{-2/3})$] finite-n terms in the edge ballooning expansion, and that both ELITE and most low-n codes do not cross the separatrix.

A series of H–mode experiments on the DIII–D tokamak exhibits a strong dependence of edge localized mode (ELM) behavior on plasma shape [1,5]. Similar observations have been made on other tokamaks and are summarized in Ref. [6]. Here we focus on a set of experiments in which the squareness (δ_2) of the plasma cross section is modified. At moderate values of $0.05 \lesssim \delta_2 \lesssim 0.2$, large infrequent ELMs are generally observed, together with a large value of the edge pressure gradient. In sharp contrast, high squareness ($\delta_2 \sim 0.5$) discharges generally produce low amplitude, high frequency ELMs, and smaller edge pressure gradients.

Low-n stability analysis has been carried out on a series of model equilibria designed to closely match the experiment [1], using a procedure outlined in [7]. A hyperbolic tangent pressure profile is employed in the edge region, with a maximum pressure gradient (p') at normalized poloidal flux $\psi = 0.96$. The edge current is set equal to the predicted bootstrap current. Low-n modes ($n < 8$) are found to be stable for the observed range of $2 \lesssim p' \backslash(10^5$ Pa/Wb$) \lesssim 3$ for the high squareness, high frequency ELM cases. However, the moderate squareness cases with large ELMs are observed to approach the low-n stability boundaries. Values of $5 \lesssim p' \lesssim 10$ are observed, near the low-n stability boundaries for $5 \lesssim n \lesssim 10$ [1].

Conventional infinite-n ballooning analysis for a typical case is shown in Fig. 1. While the high squareness edge pressure gradient is up against the ballooning limit, the moderate squareness edge has access to the second stability regime, and its pressure gradient is apparently not limited by ballooning modes.

At the plasma edge, coupling of ballooning and peeling modes can be important; in addition, finite-*n* effects may play an important role for the modes of interest ($n \lesssim 40$). The peeling mode[2,8] is a current-driven instability localized near the plasma-vacuum interface. Its stability is a strong function of the proximity of the nearest vacuum rational surface (where the safety factor $q = q_{0_{vac}}$) to the plasma edge ($q = q_a$), quantified by $\Delta = n\,(q_{0_{vac}} - q_a)$. At small values of Δ, the peeling mode is destabilized by an edge current density, and its coupling to ballooning modes can cut off access to the second stability regime. This coupling has been studied in an s–α geometry with shaping modeled by a magnetic well parameter $d_m = D_m\, s^2/\alpha$. With “poor” shaping (small negative d_m), the peeling and

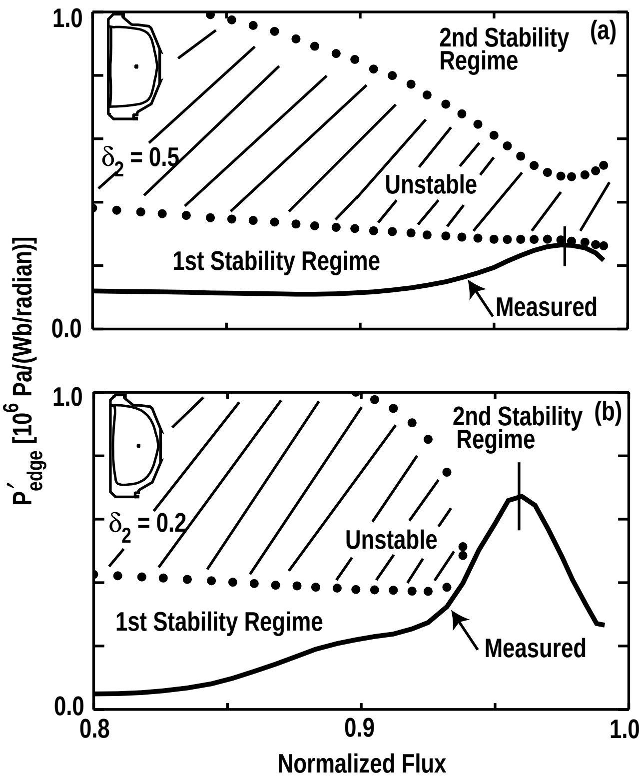

Fig. 1. Measured edge pressure gradient, and infinite-n conventional ballooning stability boundaries (a) during high frequency ELMs in a high squareness (δ_2 = 0.5) discharge and (b) during low frequency ELMs in a moderate squareness case (δ_2 = 0.2).

and ballooning modes strongly couple and prevent second stability access, while with larger negative d_m , second stability access is possible [3]. Peeling/ballooning coupling is also a function of *n*, as shown in Fig. 2(a). Higher *n* modes decouple most easily, leading to the supposition that the most unstable mode is approximately the highest *n* without second stability access (provided that *n* is low enough that it is not strongly stabilized by finite Larmor radius effects). The coupling is a very strong function of shaping as illustrated in Fig. 2(b). Over a very small range of d_m values the plasma changes from having essentially no second regime access to having access for all $n \gtrsim 10$.

For detailed comparisons to experiment, the edge ballooning equations must be solved in realistic, non-local geometry. Here the same equilibria employed in the low-*n* study [1] are evaluated for edge ballooning/peeling stability with the ELITE code. For the moderate squareness case, no extended ballooning type instabilities are seen, even when p' exceeds the low-*n* threshold. A highly localized [Fig. 3(a)] peeling instability is seen only at very low values of Δ. The critical Δ for this instability is only a very weak function of *n* and, as expected, it scales with the normalized edge current ($j_{||_a}/\langle j \rangle$) (Fig. 4). High-*n* modes are thus unstable in this case only when nq_a passes very near a rational value, and even then the mode is so strongly localized to the edge that it is unlikely to have a significant impact.

For the high squareness case, a coupled peeling/ballooning instability is seen. The mode has a predominant ballooning character, and extends over the entire high gradient region ($\psi \gtrsim 0.94$), as shown in Fig. 3(b).

These results support the following hypothesis regarding ELM character (similar to that suggested in Ref. [1]). When the H–mode edge is unstable to extended ballooning-like modes

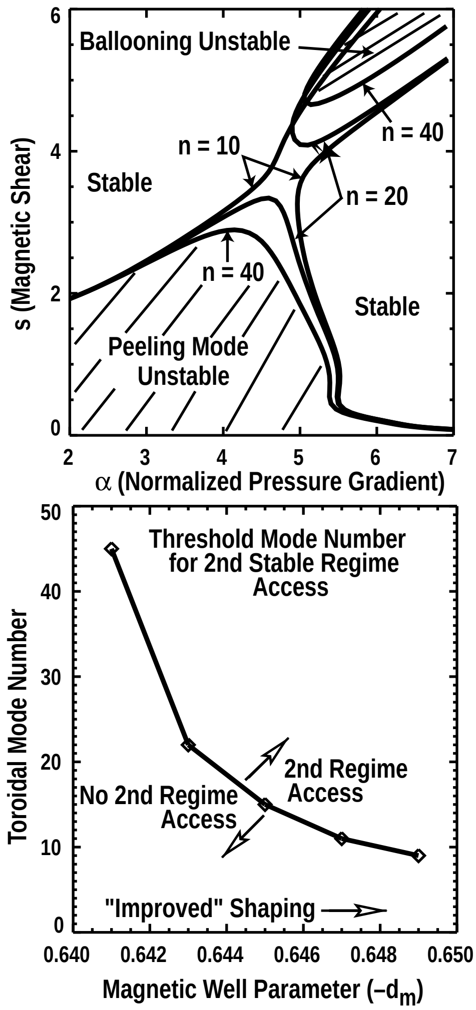

Fig. 2. (a) Stability boundaries of s–α equilibria for coupled peeling/ballooning modes at n =10,20,40, d_m = –0.645. (b) Calculated marginal value of n for second stability access, as a function of the magnetic well parameter (d_m).

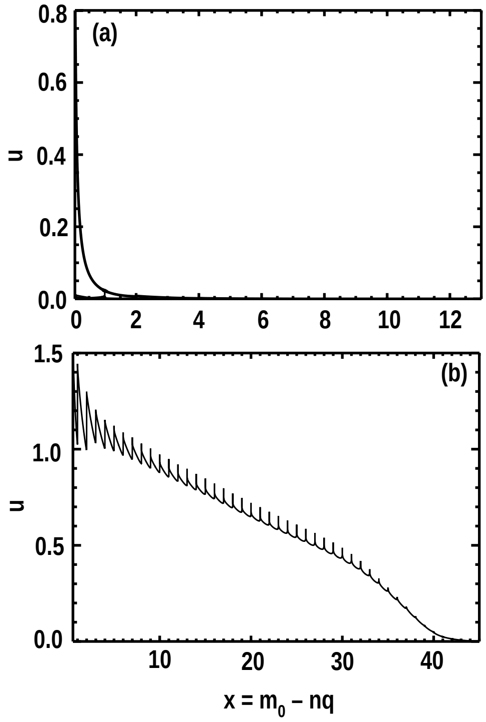

Fig. 3. Radial mode displacement (u) in: (a) the moderate squareness case (δ_2 = 0.05), Δ = 0.05, (b) the high squareness case (δ_2 = 0.5), Δ = 0.05. x = $m_{0_{vac}}$ – nq is a measure of radial location which increases from zero at the innermost vacuum rational surface to ~40 at the top of the H–mode pedestal.

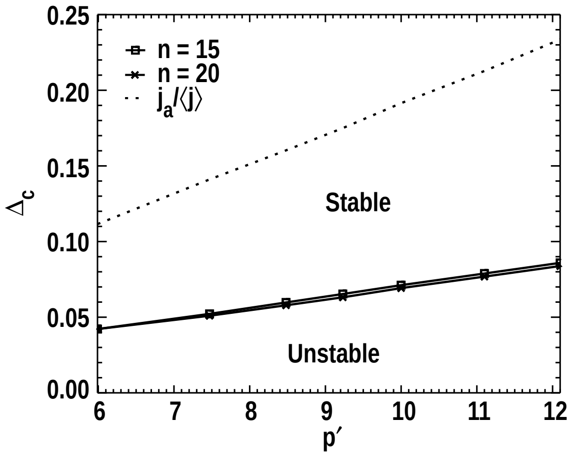

Fig. 4. Critical value of Δ for instability to peeling modes, as a function of the pressure gradient, using model equilibria with squareness δ_2 = 0.05, n = 15,20. Also shown is the normalized edge current ($j_{||a}/\langle j \rangle$).

across the steep gradient region, turbulent transport driven by these modes can, in many cases, hold p' below the low-n limit. The high-n mode turbulence results in the relatively steady fluctuations identified as small, high-frequency ELMs. However, if the equilibrium provides access to the second stability regime for coupled peeling/ballooning modes, the edge pressure gradient can rise to large values. High-n peeling modes may go unstable at small Δ, but these do not extend far enough into the plasma to relax p', which will continue to rise until a relatively low-n kink mode, with a mode structure extending across the pedestal, is driven unstable. This radially extended, fast-growing mode rapidly destroys edge confinement, resulting in a large ELM.

This picture is consistent with nonlinear simulations of turbulence driven by ballooning modes and their kinetic and resistive analogs [9–10] which find that these modes can evolve into a saturated, turbulent state with large transport. However, the evolution of the current profile is not well understood. It is possible that ballooning turbulence does not allow sufficient current relaxation, resulting in the current build-up and crash model of ELMs proposed in Ref. [2].

A number of other factors, including non-ideal effects and separatrix geometry, may impact ELMs, and nonlinear simulations are ultimately needed to understand the detailed evolution of ELMs and profiles in different regimes. These issues are beginning to be explored via an extension of the BOUT boundary turbulence code[10]. BOUT evolves the nonlinear electromagnetic Braginskii equations in separatrix geometry, modeling both the plasma edge and scrape-off layer. Parallel current terms, which are likely to be important for a full understanding of ELMs, have recently been added to the code, and preliminary simulations with edge current have been undertaken. Figure 5 shows the structure of the electrostatic potential (ϕ) in the linear phase of evolution, for a ballooning unstable equilibrium. The peaks in ϕ near the top and bottom of the machine highlight the impact of X–point geometry on these modes.

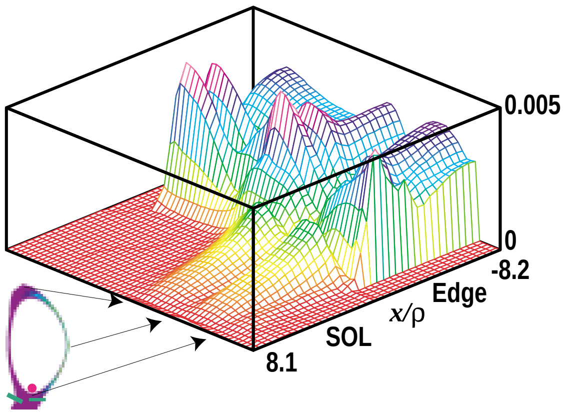

Fig. 5. Contour plot of the electrostatic potential vs. the normalized radial (x) and poloidal coordinates, in the linear phase of a BOUT simulation with current.

This is a report of work supported by the U.S. Department of Energy under Contract Nos. DE-FG03-95ER54309 and W-7405-ENG-48, and the UK Department of Trade and Industry, and Euratom. The authors wish to thank R.L. Miller for the use of his codes and G.D. Porter for his assistance with edge equilibria.

[1] J.R. Ferron, M.S. Chu, G.L. Jackson, et al., Phys. Plasmas **7**, 1976 (2000).
[2] J. Connor, R. Hastie, H.R. Wilson, and R.L. Miller, Phys. Plasmas **5**, 2687 (1998).
[3] H.R. Wilson, J. Connor, A. Field, et al., Phys. Plasmas **6**, 1925 (1999).
[4] H.R. Wilson and R.L. Miller, Phys. Plasmas **6**, 873 (1999).
[5] T.H. Osborne, J.R. Ferron, R.J. Groebner, et al., Plasma Phys. and Contr. Fusion **42**, A175 (2000).
[6] W.W. Suttrop, Plasma Phys. and Contr. Fusion **42**, A1 (2000).
[7] R.L. Miller, M.S. Chu, J.M. Greene, Y.R. Lin-Liu, and R.E. Waltz, Phys. Plasmas **5**, 973 (1998).
[8] D. Lortz, Nucl. Fusion **15**, 49 (1975).
[9] P.B. Snyder, G.W. Hammett, M.A. Beer, and W. Dorland, "Simulations of electromagnetic turbulence and transport in tokamak plasmas," in Proc. of the 26th EPS Conf. on Contr. Fusion and Plasma Phys., Maastrict, The Netherlands, 1999 (European Physical Society, 1999) ECA **23**, p. 1685.
[10] X. Xu, R. Cohen, G.D. Porter, et al., Nucl. Fusion **40**, 731 (2000).
[11] A. Zeiler, D. Biskamp, J.F. Drake, and B.N. Rogers, Phys. Plasmas **5**, 2654 (1998).